Acta Mech 223, 2647–2665 (2012)
DOI 10.1007/s00707-012-0732-y

Peijian Chen · Shaohua Chen · Zhilong Peng

Thermo-contact mechanics of a rigid cylindrical punch sliding on a finite graded layer

Received: 26 March 2012 / Revised: 14 August 2012 / Published online: 29 September 2012

Abstract A steady-state thermo-contact model of a rigid insulated cylinder of radius R sliding on a finite graded elastic layer is studied, whose Young's modulus, thermal conductivity coefficient and thermal expansion coefficient vary exponentially in the thickness direction. The transfer matrix method and Fourier integral transform technique are used to obtain a Cauchy-type singular integral equation for the contact stresses. Numerical calculation yields the interface traction and temperature distributions below the rigid punch. It shows that crack damage in the finite graded layer due to the frictional sliding can be prevented by several alternative ways, such as decreasing the shear modulus ratio of the surface to the bottom, decreasing the friction coefficient, increasing the thickness of the finite graded layer, increasing the thermal conductivity coefficient ratio of the surface to the bottom or increasing the sliding velocity. The finding should be very useful for the design of novel graded materials with potential applications in aerospace, tribology, coatings, etc.

1 Introduction

Functionally graded materials (FGMs) are special multiphase composites with continuously varying volume fractions in the thickness direction and consequently complex thermo-mechanical properties [1]. Used as coatings and interfacial zones, FGMs are found experimentally to reduce thermally and mechanically induced stresses, which result from the material mismatch [2]. Controlled gradients in material properties can also improve surface mechanical ones, such as contact damage and surface adhesion. The elastic properties of a graded material were measured by Suresh et al. [3,4], Jorgensen et al. [5], and Krumova et al. [6] experimentally with the indentation method. The elastic modulus of such a graded material can be denoted by different variation laws to describe the graded properties in the thickness direction, such as an exponential or a power law.

As a basis of the contact mechanics for graded materials, an axis-symmetric model of a graded half-space subjected to a concentrated force or an axis-symmetric indenter was considered by Giannakopoulos and Suresh [7,8]. The results show that controlling gradient variations of the substrate could alter the contact tractions, even lead to a compressive Hertzian crack at the contact edges. The same conclusions were further made via spherical indentation experiments and FEM simulations [9–11]. Closed-form solutions to a two-dimensional contact between a rigid cylinder and an elastic graded half-space were given by Giannakopoulos and Pallot [12]. Guler and Erdogan [1,13,14] investigated a frictional contact model between a rigid punch and a substrate coated with FGM and the one between two deformable elastic solids with graded coatings. Linear multilayered models were used to analyze the plane and axis-symmetric contact problems of FGM [15,16]. Receding contact between a graded coating and a homogeneous substrate as well as a partial slip contact was investigated by

P. Chen · S. Chen (✉) · Z. Peng
LNM, Institute of Mechanics, Chinese Academy of Sciences, Beijing, 100190, China
E-mail: chenshaohua72@hotmail.com

El-Borgi et al. [17] and Elloumi et al. [18]. Choi and Paulino [19] analyzed the coupled crack/contact model for a coating/substrate system with graded properties.

All the above models on graded materials belong to Hertz-type ones. Several typical studies should be mentioned for the adhesive contact of graded materials. A plane strain adhesive contact model of a rigid cylinder on an elastic graded substrate was discussed by Giannakopoulos and Pallot [12]. Chen et al. [20] further studied the corresponding axis-symmetric model and gave a very simple closed-form analytical solution for the contact of a rigid sphere on a graded elastic half-space. The problem with a flaw tolerant adhesive interface between a rigid punch and a graded half-space was investigated by Chen and Chen [21]. Non-slipping plane strain and axis-symmetric adhesive contact models were further analyzed by Jin and Guo [22] and Guo et al. [23].

Neither the above Hertz-type contact models nor adhesive ones considered thermal effects. However, it is well known that heat may show significant influence on the contact interface. Frictional heating generation will be a subject of concern to us when conventional ferrous materials are used in automotive brakes and clutches [24–27]. When brakes are applied to a moving system, the kinetic energy will be transformed into heat energy, which does not dissipate fast enough into the air stream. As a result, high temperatures and thermal stresses will produce disadvantageous effects such as surface cracks or permanent distortions [28,29]. The pressure between contact surfaces may also be affected by the thermal effect. Due to the urgent requirement of avoiding contact damage in industries, FGMs are an alternative to replace conventional materials.

Extensive studies on the thermoelastic contact problem of conventional homogeneous materials have been done [30–35]. Barber and his collaborators [36,37] have shown that, for a thermoelastic contact model, pronounced differences from an isothermal one can be found. Steady sliding of a conducting cylinder over an insulating half-plane always results in a narrower contact width comparing to the isothermal problem. Furthermore, they studied the contact problem of an insulating rigid flat-ended punch on a thermally conducting half-plane and analyzed a more general problem of a thermal conducting cylinder sliding over the surface of an elastic half-plane with different thermal properties [38]. An interesting phenomenon is that, when sufficient frictional heat is produced between two contacting bodies, the two solids may separate from each other due to the thermal effect [39,40], which has been successfully explained by Afferrante and Ciavarella [41,42].

Very limited literature is available concerning thermoelastic contacts for FGMs. Barik et al. [28] considered the contact problem of a functionally graded heat-conducting punch and a rigid insulated half-space. Choi and Paulino [43] analyzed the thermoelastic contact of a flat punch sliding over a sandwich structure, that is, a homogeneous coating on a homogeneous half-space with a graded interlayer. Liu et al. [35] investigated a thermoelastic sliding frictional contact model of a graded coated half-plane, in which the effects of the gradient index, Peclet number and the friction coefficient on the thermoelastic contact features are discussed in detail.

In the above thermal-contact models, an infinite half-space is always involved. In fact, natural objects have finite scales. In addition, contact solutions to a problem with a half-space can be achieved from the model with a finite substrate, if the thickness of the substrate tends to be infinite, while the solution to the problem with a half-space cannot be reduced generally to the one with a finite substrate. Therefore, it is necessary to establish mechanical models with finite scales and consider the boundary effects on the mechanical properties [44–47].

The present paper is aimed to develop a thermo-elastic contact model of a finite graded layer, which has so far largely been limited to an infinite graded half-space. In our model, the rigid punch is insulated and slides on the surface of the finite graded layer with heat generated in the contact region due to the interface friction. Due to the finite thickness of the graded layer, boundary effects will be paid much attention in the following analysis.

2 Formulation of the thermal-elastic contact model

To investigate the boundary effect on the contact properties, we consider a plane strain contact model as shown in Fig. 1. A rigid cylindrical punch of radius R contacts a finite graded layer of thickness h, which is fixed on a rigid foundation. The layer is assumed to be elastic and thermal conducting. The rigid insulated cylinder is subjected to a normal force P and moves from the left to the right with a constant velocity V, which yields a frictional tangential force Q in the contact region abiding by the Coulomb-type law

$$Q = \mu_{\mathrm{f}} P, \tag{1}$$

where μ_{f} is the friction coefficient and assumed to be a constant.

The problem is formulated in a coordinate system (x,y), where the y-axis is fixed on the punch and moves with the punch. It follows that the contact region, that is, $-b \le x \le a$ will remain stationary with respect to

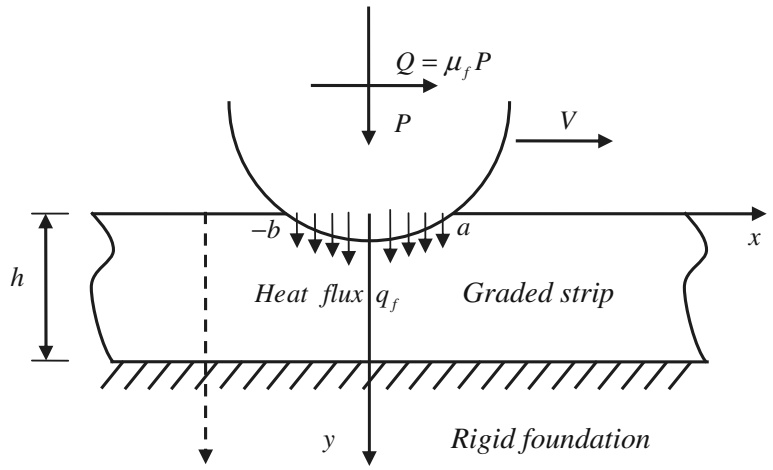

Fig. 1 Schematic of a plane strain thermoelastic contact model involving a rigid cylindrical punch of contact width $(a + b)$ sliding at a speed V on a finite graded layer of thickness h fixed on a rigid foundation. Heat transfer due to friction at the contact interface is considered with a heat flux q_{f}

the punch. Due to the sliding motion of the punch, a frictional heat flux q_{f} is generated in the contact area, which is assumed to flow only into the graded layer.

The thermal conductivity coefficient $k(y)$, shear modulus $\mu(y)$, and the thermal expansion coefficient $\alpha(y)$ of the graded layer are assumed to vary with the layer thickness according to different exponential laws as follows:

$$k_2(y) = k_1 e^{\delta y}, \quad \mu_2(y) = \mu_1 e^{\beta y}, \quad \alpha_2(y) = \alpha_1 e^{\gamma y}, \quad 0 \le y \le h, \tag{2}$$

$$\delta = \frac{1}{h}\ln\left(\frac{k_3}{k_1}\right), \quad \beta = \frac{1}{h}\ln\left(\frac{\mu_3}{\mu_1}\right), \quad \gamma = \frac{1}{h}\ln\left(\frac{\alpha_3}{\alpha_1}\right), \tag{3}$$

where the subscript "1" denotes the surface of the graded layer $y = 0$, "2" denotes the inside region and "3" the lower boundary $y = h$. The Poisson's ratio ν of the graded layer is assumed to be a constant.

$u(x, y)$ and $v(x, y)$ are displacement components in the x- and y-directions, respectively. $T(x, y)$ is the temperature field measured from a referenced stress-free temperature. The constitutive relations for the graded layer in terms of $u(x, y)$, $v(x, y)$ and $T(x, y)$ can be given as

$$\sigma_{xx} = \frac{\mu_2}{\kappa - 1}\left[(1+\kappa)\frac{\partial u}{\partial x} + (3-\kappa)\frac{\partial v}{\partial y} - 4\alpha_2^* T\right], \tag{4a}$$

$$\sigma_{yy} = \frac{\mu_2}{\kappa - 1}\left[(1+\kappa)\frac{\partial v}{\partial y} + (3-\kappa)\frac{\partial u}{\partial x} - 4\alpha_2^* T\right], \tag{4b}$$

$$\tau_{xy} = \mu_2\left[\frac{\partial u}{\partial y} + \frac{\partial v}{\partial x}\right]. \tag{4c}$$

where $\kappa = 3 - 4\nu$, $\alpha_j^* = (1+\nu)\alpha_j$, $(j = 1, 2, 3)$ for a plane strain problem and $\kappa = (3-\nu)/(1+\nu)$, $\alpha_j^* = \alpha_j$, $(j = 1, 2, 3)$ for a plane stress one.

According to Barik et al. [28], Choi and Paulino [43], Jang and Ahn [29], Pauk [31], and Zhou and Lee [48], the steady-state heat conduction equation of the graded layer can be given as

$$\frac{\partial^2 T}{\partial x^2} + \frac{\partial^2 T}{\partial y^2} + \delta\frac{\partial T}{\partial y} = 0. \tag{5}$$

In the present thermal-elastic sliding-contact problem, we only consider the sliding velocity much slower than the Rayleigh wave speed of the graded layer. Thus, the inertia effects could be neglected [35,49], which leads to the following equilibrium equations:

$$\nabla^2 u + \frac{2}{\kappa - 1}\left(\frac{\partial^2 u}{\partial x^2} + \frac{\partial^2 v}{\partial x \partial y}\right) + \beta\left(\frac{\partial u}{\partial y} + \frac{\partial v}{\partial x}\right) = \frac{4\alpha_2^* e^{\gamma y}}{\kappa - 1}\frac{\partial T}{\partial x}, \tag{6a}$$

$$\nabla^2 v + \frac{2}{\kappa - 1}\left(\frac{\partial^2 v}{\partial y^2} + \frac{\partial^2 u}{\partial x \partial y}\right) + \frac{\beta}{\kappa - 1}\left[(1+\kappa)\frac{\partial v}{\partial y} + (3-\kappa)\frac{\partial u}{\partial x}\right] = \frac{4\alpha_2^* e^{\gamma y}}{\kappa - 1}\left[(\beta + \gamma)T + \frac{\partial T}{\partial y}\right]. \tag{6b}$$

The governing equations for the present model consist of Eqs. (5) and (6). For a special case of a homogeneous layer, we have $\delta = 0, \beta = 0, \gamma = 0$.

2.1 Mechanical boundary conditions

For a plane strain model with a cylindrical punch, the normal displacement within the contact area is

$$u(x, 0) = \delta_0 - \frac{x^2}{2R}, \quad \frac{\partial u(x, 0)}{\partial x} = -\frac{x}{R}, \quad -b \le x \le a, \tag{7}$$

where δ_0 is the vertical translation of the rigid cylindrical punch and $x^2/2R$ comes from the parabolic assumption of the rigid cylinder profile [50]. Usually, the effect of gravity is neglected [43,51]. The normal and tangential tractions beneath the punch abide by the Coulomb friction law and the applied indentation force P equal to the integral of the interface normal stress, that is,

$$\sigma_{xy}(x, 0) = \mu_f \sigma_{yy}(x, 0), \quad -b \le x \le a, \tag{8}$$

$$\int_{-b}^{a} \sigma_{yy}(x, 0)\,\mathrm{d}x = -P, \quad -b \le x \le a. \tag{9}$$

Outside the contact region, the normal and tangential stresses vanish, that is, a free boundary,

$$\sigma_{yy}(x, 0) = \sigma_{xy}(x, 0) = 0, \quad x < -b, x > a. \tag{10}$$

It is assumed that the graded layer is fixed on a rigid substrate. Thus, the boundary condition of the normal and tangential displacements at $y = h$ can be expressed as

$$u(x, h) = v(x, h) = 0. \tag{11}$$

2.2 Thermal boundary conditions

In view of the fact that the frictional heat flows only into the graded layer through the contact area without any loss to the surroundings [37], the problem is treated within the linear thermoelasticity framework. According to Joachim-Ajao and Barber [52], the heat flux generated by the tangential traction inside the contact area is modeled to equal the generating rate of frictional heat,

$$k_1 \frac{\partial T(x, 0)}{\partial y} = -q_f(x), \quad -b \le x \le a, \tag{12}$$

where $q_f(x)$ is the heat flux depending on the sliding velocity V, the friction coefficient μ_f and the interface normal stress σ_{yy},

$$q_f(x) = -\mu_f V \sigma_{yy}(x, 0). \tag{13}$$

The area outside the contact region is thermally insulated, that is,

$$k_1 \frac{\partial T(x, 0)}{\partial y} = 0, \quad x < -b, \quad x > a. \tag{14}$$

It is assumed that the temperature on the lower surface of the graded layer is identical to the environmental one. Then, the relative temperature at $y = h$ can be written as

$$T(x, h) = 0, \quad |x| < \infty. \tag{15}$$

2.3 Temperature and displacement fields

In order to solve the thermoelastic governing equations in Eqs. (5) and (6) and obtain the temperature and displacement fields, the Fourier integral transform method, as a standard technique, can be employed.

Transform with respect to x in Eq. (5) leads to the temperature field,

$$T(x, y) = \frac{1}{2\pi} \int_{-\infty}^{+\infty} \sum_{j=1}^{2} A_j e^{\lambda_j y - \mathrm{i}sx} \mathrm{d}s, \tag{16}$$

where s is a transform variable, $\mathrm{i}^2 = -1$ and $\lambda_i(s)$ $(j = 1, 2)$ are given as

$$\lambda_1 = -\frac{\delta}{2} + \sqrt{\frac{\delta^2}{4} + s^2}, \quad \lambda_2 = -\frac{\delta}{2} - \sqrt{\frac{\delta^2}{4} + s^2}. \tag{17}$$

$A_j(s)$, $j = 1, 2$, as unknown functions, can be determined by the thermal and interface boundary conditions in Eqs. (12)–(15):

$$A_1 = \frac{\bar{q}_{\mathrm{f}} e^{\lambda_2 h}}{\lambda_1 e^{\lambda_2 h} - \lambda_2 e^{\lambda_1 h}}, \quad A_2 = \frac{\bar{q}_{\mathrm{f}} e^{\lambda_1 h}}{\lambda_2 e^{\lambda_1 h} - \lambda_1 e^{\lambda_2 h}}, \tag{18}$$

where

$$\bar{q}_{\mathrm{f}}(s) = -\int_{-b}^{a} \frac{q_{\mathrm{f}}(\xi)}{k_1} e^{\mathrm{i}s\xi} \mathrm{d}\xi. \tag{19}$$

Using the Fourier integral transform method, Eqs. (6a) and (6b) yield the displacement fields

$$u = \frac{1}{2\pi} \int_{-\infty}^{+\infty} \sum_{j=1}^{4} B_j e^{m_j y - \mathrm{i}sx} \mathrm{d}s + \frac{4\alpha_2^* e^{\gamma y}}{\kappa - 1} \frac{\mathrm{i}}{2\pi} \int_{-\infty}^{+\infty} \sum_{j=1}^{2} A_j \frac{\Omega_j}{\Delta_j} e^{\lambda_j y - \mathrm{i}sx} \mathrm{d}s, \tag{20}$$

$$v = -\frac{\mathrm{i}}{2\pi} \int_{-\infty}^{+\infty} \sum_{j=1}^{4} B_j F_j e^{m_j y - \mathrm{i}sx} \mathrm{d}s + \frac{4\alpha_2^* e^{\gamma y}}{\kappa - 1} \frac{1}{2\pi} \int_{-\infty}^{+\infty} \sum_{j=1}^{2} A_j \frac{\Phi_j}{\Delta_j} e^{\lambda_j y - \mathrm{i}sx} \mathrm{d}s, \tag{21}$$

where

$$\Omega_j = s\left(\beta + \gamma + \lambda_j\right)\left[W_j + 2\beta\left(\frac{\kappa - 2}{\kappa - 1}\right)\right] - sD_j, \tag{22a}$$

$$\Phi_j = \left(\beta + \gamma + \lambda_j\right)\left[\left(\frac{\kappa - 1}{\kappa + 1}\right) D_j - \frac{4\kappa s^2}{\kappa^2 - 1}\right] + s^2 W_j, \tag{22b}$$

$$\Delta_j = \left[\left(\frac{\kappa - 1}{\kappa + 1}\right) D_j - \frac{4\kappa s^2}{\kappa^2 - 1}\right] D_j + s^2\left[W_j + 2\beta\left(\frac{\kappa - 2}{\kappa - 1}\right)\right] W_j, \tag{22c}$$

and

$$D_j = \left(\frac{\kappa + 1}{\kappa - 1}\right)\left(\gamma + \lambda_j\right)\left(\beta + \gamma + \lambda_j\right) - s^2, \tag{23a}$$

$$W_j = \frac{2\left(\gamma + \lambda_j\right) + \beta\left(3 - \kappa\right)}{\kappa - 1}. \tag{23b}$$

$B_j(s)$ in Eqs. (20) and (21) is an arbitrary unknown, which can be determined by the mechanical boundary conditions in Eqs. (8)–(11). $m_j(s)$ is the root of the following characteristic equation:

$$\left(m^2 - s^2 + \beta m\right)^2 + \left(\frac{3 - \kappa}{1 + \kappa}\right) s^2 \beta^2 = 0. \tag{24}$$

Solving Eq. (24) results in

$$m_j = -\frac{\beta}{2} + \sqrt{\frac{\beta^2}{4} + s^2 - \mathrm{i}\,(-1)^j\,\beta s \left(\frac{3-\kappa}{1+\kappa}\right)^{1/2}}, \qquad Re\left(m_j\right) > 0, \quad j = 1, 2, \tag{25a}$$

$$m_j = -\frac{\beta}{2} - \sqrt{\frac{\beta^2}{4} + s^2 + \mathrm{i}\,(-1)^j\,\beta s \left(\frac{3-\kappa}{1+\kappa}\right)^{1/2}}, \qquad Re\left(m_j\right) < 0, \quad j = 3, 4, \tag{25b}$$

and $F_j\,(s)$ can be expressed as a function of $m_j\,(s)$ as follows:

$$F_j = \frac{(\kappa-1)\left(m_j^2 + \beta m_j\right) - s^2\,(\kappa+1)}{s\left[2m_j + \beta\,(\kappa-1)\right]} \quad (j = 1, \ \ldots, \ 4)\,. \tag{26}$$

3 Transfer matrix approach for the problem

In order to find the displacements of a graded layer subjected to arbitrary tractions and heat flux, a transfer matrix approach can be employed.

From the general solutions in Eqs. (20) and (21) and the constitutive relations in Eqs. (4a–c), the displacements and tractions of the graded layer can be written in a Fourier-transformed domain as

$$\mathbf{f}\,(s, y) = \mathbf{\Theta}\,(s, y)\,\mathbf{a}\,(s) + \mathbf{f}_{\mathrm{T}}\,(s, y)\,, \tag{27}$$

where $\mathbf{f}\,(s, y)$ is a state vector containing physical variables that need to be determined for the given constituents, $\mathbf{a}\,(s)$ is a vector for the four unknowns in the general solutions of the present thermoelastic contact problem as follows:

$$\mathbf{f}\,(s, y) = \left\{\bar{v}\,(s, y)/\mathrm{i}, \ \bar{u}\,(s, y)\,, \ \bar{\sigma}_{yy}\,(s, y)/\mathrm{i}, \ \bar{\tau}_{xy}\,(s, y)\right\}^T, \tag{28}$$

$$\mathbf{a}\,(s) = \{B_1\,(s)\,, \ B_2\,(s)\,, \ B_3\,(s)\,, \ B_4\,(s)\}^{\mathrm{T}}. \tag{29}$$

$\mathbf{\Theta}\,(s, y)$ is a 4×4 matrix, which is a function of not only the variables s and y, but also elastic parameters of the constituents. $\mathbf{f}_{\mathrm{T}}\,(s, y)$ is a vector representing the non-isothermal effect originating from the non-homogeneous part of the governing equations (20) and (21).

At the bottom interface $y = h$, we have

$$\mathbf{f}\,(s, h) = \mathbf{\Theta}\,(s, h)\,\mathbf{a}\,(s) + \mathbf{f}_{\mathrm{T}}\,(s, h)\,, \tag{30}$$

where

$$\mathbf{f}\,(s, h) = \left\{0, \quad 0, \quad \bar{\sigma}_{yy}\,(s, h)/\mathrm{i}, \quad \bar{\tau}_{xy}\,(s, h)\right\}^{\mathrm{T}}. \tag{31}$$

On the upper surface of the graded layer $y = 0$, we have

$$\mathbf{f}\,(s, 0) = \mathbf{\Theta}\,(s, 0)\,\mathbf{a}\,(s) + \mathbf{f}_{\mathrm{T}}\,(s, 0)\,, \tag{32}$$

where

$$\mathbf{f}\,(s, 0) = \left\{\bar{v}\,(s, 0)/\mathrm{i}, \ \bar{u}\,(s, 0)\,, \ \bar{\sigma}_{yy}\,(s, 0)/\mathrm{i}, \ \bar{\tau}_{xy}\,(s, 0)\right\}, \tag{33}$$

Here, $\bar{\sigma}_{yy}\,(s, 0)$ and $\bar{\tau}_{xy}\,(s, 0)$ denote the transformed normal and tangential tractions on the upper surface of the graded layer. Therefore

$$\bar{\sigma}_{yy}\,(s, 0) = \int_{-b}^{a} \sigma_{yy}\,(x, 0)\,e^{\mathrm{i}sx}\mathrm{d}x, \bar{\tau}_{xy}\,(s, 0) = \int_{-b}^{a} \tau_{xy}\,(x, 0)\,e^{\mathrm{i}sx}\mathrm{d}x. \tag{34}$$

Eliminating the unknown vector $\mathbf{a}\,(s)$ in Eqs. (30) and (32) yields

$$\mathbf{f}\,(s, 0) = \mathbf{G}\,(s)\,\mathbf{f}\,(s, h) + \mathbf{r}_0, \tag{35}$$

where $\mathbf{G}(s)$ is a 4×4 transfer matrix connecting the upper and the lower surfaces of the graded layer and $\mathbf{r}_0(s)$ is a vector of length four involving the thermal loading,

$$\mathbf{G}(s) = \mathbf{\Theta}(s,0)\,\mathbf{\Theta}^{-1}(s,h), \tag{36a}$$

$$\mathbf{r}_0 = -\mathrm{i}\mathbf{r}(s)\,\bar{q}_\mathrm{f} = -\mathbf{\Theta}(s,0)\,\mathbf{\Theta}^{-1}(s,h)\,\mathbf{f}_\mathrm{T}(s,h) + \mathbf{f}_\mathrm{T}(s,0), \tag{36b}$$

The superscript "-1" denotes the inverse of a matrix.

Thus, the transformed surface displacements $\bar{u}(s,0)$ and $\bar{v}(s,0)$ can be achieved in terms of the transformed surface tractions $\bar{\sigma}_{yy}(s,0)$, $\bar{\tau}_{xy}(s,0)$, and the heat flux $\bar{q}_\mathrm{f}$. Inverse Fourier transform leads to the following integral equations, where the surface displacements are functions of the surface tractions,

$$v(x,0) = \frac{1}{2\pi}\int_{-\infty}^{+\infty}\left[N_{11}(s)\,\bar{\sigma}_{yy}(s,0) + \mathrm{i}N_{12}(s)\,\bar{\tau}_{xy}(s,0) + L_1(s)\,\bar{q}_\mathrm{f}\right]\mathrm{e}^{-isx}\mathrm{d}s, \quad |x| < +\infty, \tag{37}$$

$$u(x,0) = \frac{1}{2\pi}\int_{-\infty}^{+\infty}\left[-\mathrm{i}N_{21}(s)\,\bar{\sigma}_{yy}(s,0) + N_{22}(s)\,\bar{\tau}_{xy}(s,0) - \mathrm{i}L_2(s)\,\bar{q}_\mathrm{f}\right]\mathrm{e}^{-isx}\mathrm{d}s, \quad |x| < +\infty, \tag{38}$$

where $N_{jk}(s)\,(j,k=1,2)$ are elements of a 2×2 matrix $\mathbf{N}(s)$; $L_j(s)\,(j=1,2)$ are those of a vector of two units in length $\mathbf{L}(s)$,

$$\mathbf{N}(s) = \begin{bmatrix} G_{13} & G_{14} \\ G_{23} & G_{24} \end{bmatrix}\begin{bmatrix} G_{33} & G_{34} \\ G_{43} & G_{44} \end{bmatrix}^{-1}, \tag{39}$$

$$\mathbf{L}(s) = \begin{Bmatrix} r_1 \\ r_2 \end{Bmatrix} - \begin{bmatrix} G_{13} & G_{14} \\ G_{23} & G_{24} \end{bmatrix}\begin{bmatrix} G_{33} & G_{34} \\ G_{43} & G_{44} \end{bmatrix}^{-1}\begin{Bmatrix} r_3 \\ r_4 \end{Bmatrix}. \tag{40}$$

It is found that $\mathbf{N}(s)$ depends only on the elastic parameters of the constituents of the graded layer, while $\mathbf{L}(s)$ depends on thermoelastic parameters of such constituents.

4 Solution of the integral equations

Considering Eqs. (19) and (34) and differentiating with respect to the variable x, the integral equations (37) and (38) can be rewritten as

$$\frac{\partial v(x,0)}{\partial x} = -\frac{1}{2\pi}\int_{-b}^{+a}\left[\mathrm{i}I_{11}(x,r)\,\sigma_{yy}(r,0) - I_{12}(x,r)\,\tau_{xy}(r,0) + \mathrm{i}I_{13}(x,r)\,q_\mathrm{f}(r)\right]\mathrm{d}r, \tag{41}$$

$$\frac{\partial u(x,0)}{\partial x} = -\frac{1}{2\pi}\int_{-b}^{+a}\left[I_{21}(x,r)\,\sigma_{yy}(r,0) + \mathrm{i}I_{22}(x,r)\,\tau_{xy}(r,0) + I_{23}(x,r)\,q_\mathrm{f}(r)\right]\mathrm{d}r, \tag{42}$$

where the kernels are

$$I_{jk}(x,r) = \int_{-\infty}^{+\infty} sN_{jk}(\mathrm{s})\,\mathrm{e}^{is(r-x)}\mathrm{d}s, \quad j=1,2,k=1,2, \tag{43}$$

$$I_{j3}(x,r) = -\frac{1}{k_1}\int_{-\infty}^{+\infty} sL_j(\mathrm{s})\,\mathrm{e}^{is(r-x)}\mathrm{d}s, \quad j=1,2. \tag{44}$$

For a large value of $|s|$, we have the following asymptotic solutions:

$$\lim_{|s|\to\infty} sN_{11} = \Lambda_{11}\frac{s}{|s|},\ \lim_{|s|\to\infty} sN_{22} = \Lambda_{22}\frac{s}{|s|}, \tag{45a}$$

$$\lim_{|s|\to\infty} sN_{12} = \Lambda_{12},\ \lim_{|s|\to\infty} sN_{21} = \Lambda_{21}, \tag{45b}$$

$$\lim_{|s|\to\infty} sL_1 = \lim_{|s|\to\infty} sL_2 = 0, \tag{45c}$$

where $\Lambda_{11} = \Lambda_{22} = -\frac{(\kappa+1)}{4\mu_1}$ and $\Lambda_{12} = \Lambda_{21} = -\frac{(\kappa-1)}{4\mu_1}$.

After separating the leading terms from the kernels in Eq. (45) and using the following generalized functions

$$\int_0^\infty \sin\left[s\left(r-x\right)\right]\mathrm{d}s = \frac{1}{r-x},\quad \int_0^\infty \cos\left[s\left(r-x\right)\right]\mathrm{d}s = \pi\delta\left(r-x\right), \tag{46}$$

where $\delta(\cdot)$ is the Dirac delta function, Eqs. (41) and (42) can be written as

$$\frac{\partial v\left(x,0\right)}{\partial x} = \Lambda_{12}\tau_{xy}\left(x,\ 0\right) + \frac{1}{\pi}\int_{-b}^{a}\frac{\Lambda_{11}}{r-x}\sigma_{yy}\left(r,\ 0\right)\mathrm{d}r$$
$$+\frac{1}{\pi}\int_{-b}^{a}\left[K_{11}\left(x,r\right)\sigma_{yy}\left(r,\ 0\right) + K_{12}\left(x,r\right)\tau_{xy}\left(r,\ 0\right) - \frac{1}{k_1}K_{13}\left(x,r\right)q_{\mathrm{f}}\left(r\right)\right]\mathrm{d}r, \tag{47a}$$

$$\frac{\partial u\left(x,0\right)}{\partial x} = -\Lambda_{21}\sigma_{yy}\left(x,\ 0\right) + \frac{1}{\pi}\int_{-b}^{a}\frac{\Lambda_{22}}{r-x}\tau_{xy}\left(r,\ 0\right)\mathrm{d}r$$
$$-\frac{1}{\pi}\int_{-b}^{a}\left[K_{21}\left(x,r\right)\sigma_{yy}\left(r,\ 0\right) - K_{22}\left(x,r\right)\tau_{xy}\left(r,\ 0\right) - \frac{1}{k_1}K_{23}\left(x,r\right)q_{\mathrm{f}}\left(r\right)\right]\mathrm{d}r, \tag{47b}$$

where $K_{mn}\left(x,r\right)\left(m,n=1,2\right)$ are defined as

$$K_{mn}\left(x,r\right) = \begin{cases} \int_0^\infty \left[sN_{mn}\left(s\right) - \Lambda_{mn}\right]\sin\left[s\left(r-x\right)\right]\mathrm{d}s, & m=n, \\ \int_0^\infty \left[sN_{mn}\left(s\right) - \Lambda_{mn}\right]\cos\left[s\left(r-x\right)\right]\mathrm{d}s, & m\neq n, \end{cases} \tag{48a}$$

and

$$K_{13}\left(x,r\right) = \int_0^\infty sL_1\left(s\right)\sin\left[s\left(r-x\right)\right]\mathrm{d}s, \tag{48b}$$

$$K_{23}\left(x,r\right) = \int_0^\infty sL_2\left(s\right)\cos\left[s\left(r-x\right)\right]\mathrm{d}s. \tag{48c}$$

Considering the relations in Eqs. (8) and (13), we have

$$\sigma_{yy}\left(x,\ 0\right) = -p(x),\quad -b\le x\le a, \tag{49}$$

$$\sigma_{xy}\left(x,\ 0\right) = -\mu_{\mathrm{f}}p(x),\quad -b\le x\le a, \tag{50}$$

$$q_{\mathrm{f}}(x) = \mu_{\mathrm{f}}Vp(x),\quad -b\le x\le a, \tag{51}$$

where $p(x)$ denotes the normal traction in the contact region.

Then, Eq. (47a) can be rewritten as

$$\mu_{\mathrm{f}}\Lambda_{12}p(x) + \frac{1}{\pi}\int_{-b}^{a}\frac{\Lambda_{11}}{r-x}p\left(r\right)\mathrm{d}r + \frac{1}{\pi}\int_{-b}^{a}Q_1\left(x,r\right)p\left(r\right)\mathrm{d}r = g(x), \tag{52}$$

where the bounded kernel $Q_1(x,r)$ is

$$Q_1(x,r) = K_{11}(x,r) + \mu_f K_{12}(x,r) + \frac{\mu_f V}{k_1} K_{13}(x,r) \tag{53}$$

and $g(x)$ is given as

$$g(x) = -\frac{\partial v(x,0)}{\partial x}. \tag{54}$$

Equation (52) is a standard formula denoting the surface displacements as functions of the surface tractions, in which the effects of sliding velocity and friction heat are included in the kernel $Q_1(x,r)$.

Introducing the following normalized quantities

$$\begin{cases} r = \frac{a+b}{2}\eta + \frac{a-b}{2}, \quad x = \frac{a+b}{2}\xi + \frac{a-b}{2}, \quad -b < (r,x) < a, \quad -1 < (\eta,\xi) < 1, \\ Q^*(\xi,\eta) = \frac{a+b}{2} Q_1(\xi,\eta). \end{cases} \tag{55}$$

Equations (52) and (9) can be rewritten as

$$\mu_f \Lambda_{12} p(\xi) + \frac{1}{\pi}\int_{-1}^{1} \frac{\Lambda_{11}}{\eta-\xi} p(\eta)\,\mathrm{d}\eta + \frac{1}{\pi}\int_{-1}^{1} Q^*(\xi,\eta)\, p(\eta)\mathrm{d}\eta = g(\xi), \ |\xi| < 1, \tag{56}$$

$$\int_{-1}^{1} p(\xi)\mathrm{d}\xi = \frac{2P}{a+b}. \tag{57}$$

Due to the Cauchy-type singular kernel in the integral equation, the solution to Eqs. (56) and (57) can be expressed as a series expansion such that

$$p(\xi) = w(\xi)\sum_{j=0}^{\infty} c_j P_j^{(\beta_1,\beta_2)}(\xi), \quad |\xi| < 1, \tag{58}$$

where $w(\xi) = (1-\xi)^{\beta_1}(1+\xi)^{\beta_2}$ is a weight function, c_j denotes an unknown coefficient, $P_j^{(\beta_1,\beta_2)}(\cdot)$ is a Jacobi Polynomial corresponding to the weight function $w(\xi)$.

The superscripts β_1 and β_2 can be determined from the physics of the present model as

$$\begin{cases} \theta > 0: & \beta_1 = 1 - \frac{\varepsilon}{\pi}, & \beta_2 = \frac{\varepsilon}{\pi} \\ \theta = 0: & \beta_1 = \frac{1}{2}, & \beta_2 = \frac{1}{2} \\ \theta < 0: & \beta_1 = \frac{\varepsilon}{\pi}, & \beta_2 = 1 - \frac{\varepsilon}{\pi} \end{cases} \tag{59}$$

and $\theta = \frac{\mu_f \Lambda_{12}}{\Lambda_{11}}$, $\tan\varepsilon = |\frac{1}{\theta}|$.

It is easy to find that β_1 and β_2, as the index of stress singularity at the leading ($x = a$) and the trailing ($x = -b$) contact edges, respectively, depend on the friction coefficient and Poisson's ratio. This feature is similar to that in the corresponding isothermal problem.

Considering the following property of a Jacobi Polynomial,

$$\mu_f \Lambda_{12} w(\xi) P_j^{(\beta_1,\beta_2)}(\xi) + \frac{1}{\pi}\int_{-1}^{1} \frac{\Lambda_{11}}{\eta-\xi} w(\eta) P_j^{(\beta_1,\beta_2)}(\eta)\,\mathrm{d}\eta = -\frac{2\Lambda_{11}}{\sin(\pi\beta_1)} P_{j+1}^{(-\beta_1,-\beta_2)}(\xi), \ |\xi| < 1, \tag{60}$$

and truncating the series at $j = N$, then, substituting Eq. (58) into Eqs. (56), (57) leads to

$$\sum_{j=0}^{N}\left[\frac{-2\Lambda_{11}}{\sin(\pi\beta_1)} P_{j+1}^{(-\beta_1,-\beta_2)}(\xi) + Q_j^*(\xi)\right] c_j = g(\xi), \tag{61}$$

$$\sum_{j=0}^{N} c_j \int_{-1}^{1} w(\xi) P_j^{(\beta_1,\beta_2)}(\xi)\,\mathrm{d}\xi = \frac{2P}{a+b}, \tag{62}$$

where

$$Q_j^* (\xi) = \frac{1}{\pi} \int_{-1}^{1} Q^* (\xi, \eta) w (\eta) P_j^{(\beta_1, \beta_2)} (\eta) \, \mathrm{d}\eta. \tag{63}$$

Using the following orthogonality property of a Jacobi Polynomial

$$\int_{-1}^{1} w (\xi) P_j^{(\beta_1, \beta_2)} (\xi) P_k^{(\beta_1, \beta_2)} (\xi) \, \mathrm{d}\xi = \theta_j^{(\beta_1, \beta_2)} \delta_{jk}, \quad j, k = 0, 1, 2, \ldots, \tag{64}$$

Eqs. (61) and (62) can be recast into a set of linear algebraic equations for c_j $(0 \le j \le N-1)$,

$$\frac{-2\Lambda_{11}}{\sin (\pi \beta_1)} \theta_j^{(-\beta_1, -\beta_2)} c_{j-1} + \sum_{n=0}^{N-1} d_{jn} c_n = \Gamma_j, \quad j = 0, 1, 2, \ldots, N, \tag{65a}$$

$$c_0 \theta_0^{(\beta_1, \beta_2)} = \frac{2P}{a+b}, \tag{65b}$$

where $c_{-1} = 0$, δ_{jk} is the Kronecker delta function and

$$\theta_j^{(\beta_1, \beta_2)} = \begin{cases} \int_{-1}^{1} w (\xi) \mathrm{d}\xi = \frac{2^{\beta_1+\beta_2+1} \Gamma(\beta_1+1) \Gamma(\beta_2+1)}{\Gamma(\beta_1+\beta_2+2)}, & j = 0, \\ \frac{2^{\beta_1+\beta_2+1} \Gamma(j+\beta_1+1) \Gamma(j+\beta_2+1)}{(2j+\beta_1+\beta_2+1) j! \Gamma(j+\beta_1+\beta_2+1)}, & j \ge 1, \end{cases} \tag{66}$$

$$d_{jn} = \int_{-1}^{1} P_j^{(-\beta_1, -\beta_2)} (\xi) \, Q_j^* (\xi) \, (1+\xi)^{-\beta_1} (1-\xi)^{-\beta_2} \, \mathrm{d}\xi, \tag{67}$$

$$\Gamma_j = \int_{-1}^{1} P_j^{(-\beta_1, -\beta_2)} (\xi) \, g (\xi) \, (1+\xi)^{-\beta_1} (1-\xi)^{-\beta_2} \, \mathrm{d}\xi. \tag{68}$$

In addition, the normal contact stress should vanish at both the left and right contact edges due to a Hertzian contact considered in the present paper,

$$p (-b) = p (a) = 0, \tag{69}$$

where a and b are contact lengths as shown in Fig. 1.

For a cylindrical stamp, we have

$$g (\xi) = \frac{1}{2R} [(a+b) \xi + (a-b)]. \tag{70}$$

It should be noted that for the case of a cylindrical punch, the solution of Eqs. (56) and (57) must satisfy a consistency condition [53],

$$\int_{-1}^{1} \frac{S (\xi)}{(1-\xi)^{\beta_1} (1-\xi)^{\beta_2}} \mathrm{d}\xi = 0, \tag{71}$$

where

$$S (\xi) = \mu_{\mathrm{f}} \Lambda_{12} p (\xi) + \frac{1}{\pi} \int_{-1}^{1} \frac{\Lambda_{11}}{\eta - \xi} p (\eta) \, \mathrm{d}\eta. \tag{72}$$

According to Krenk [54], it is easy to prove that Eq. (71) is automatically satisfied in the present problem.

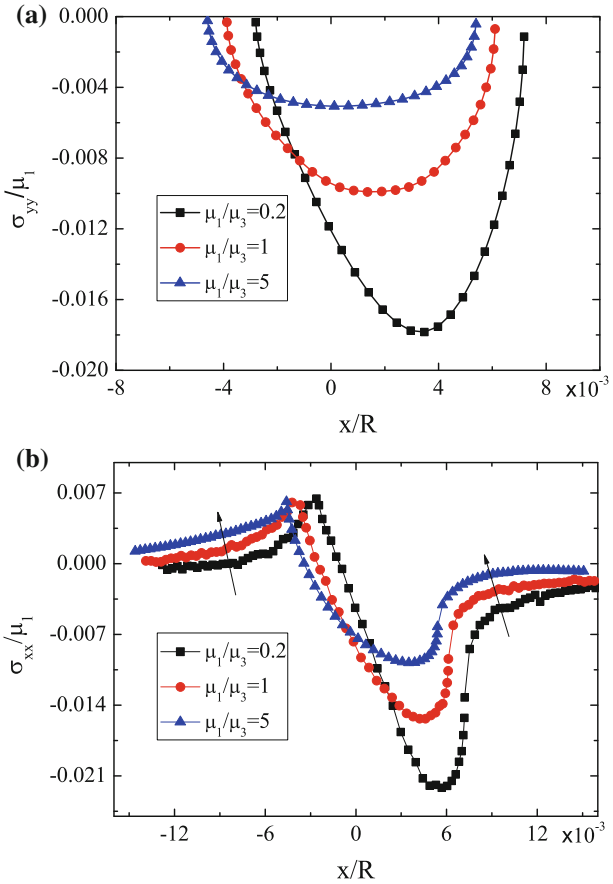

Fig. 2 Distributions of the non-dimensional contact stresses along the contact interface for different shear modulus ratios μ_1/μ_3 with fixed values $v_0 = 0.2$, $(a+b)/h = 1$, $R/h = 100$, $\mu_f = 0.5$. **a** For the contact pressure $\sigma_{yy}(x,0)/\mu_1$; **b** for the in-plane stress $\sigma_{xx}(x,0)/\mu_1$

Thus, numerical results of the present model can be obtained by solving Eqs. (65a) and (65b). Based on the solutions of Eqs. (65a) and (65b) and considering Eqs. (49) and (58), we can find $\sigma_{yy}(x,0)$,

$$\sigma_{yy}(x,0) = -(a-x)^{\beta_1}(b+x)^{\beta_2}\frac{2}{a+b}\sum_{j=0}^{N-1} c_j P_j^{(\beta_1,\beta_2)}\left(\frac{x-(a-b)/2}{(a+b)/2}\right), \quad -b \le x \le a. \tag{73}$$

Then, the stress component $\sigma_{xx}(x,0)$ below the punch can be found from the constitutive relations in Eqs. (4a)–(4b) and (47b) as

$$\sigma_{xx}(x,0) = -p(x) + \frac{2\mu_f}{\pi}\int_{-b}^{a}\frac{1}{r-x}p(r)\,\mathrm{d}r - \frac{2}{\pi}\int_{-b}^{a}\frac{1}{\Lambda_{22}}Q_2(x,r)\,p(r)\,\mathrm{d}r + \frac{2\alpha_1^*}{\Lambda_{22}}T(x,0), \ |x| < \infty, \tag{74}$$

where

$$Q_2(x,r) = K_{21}(x,r) - \mu_f K_{22}(x,r) + \frac{\mu_f V}{k_1}K_{23}(x,r). \tag{75}$$

5 Results and discussions

In the present paper, a plane strain case is assumed with a constant Poisson's ratio $\nu = 0.3$. $\alpha_1/\alpha_3 = 0.6903$, $k_1/k_3 = 0.1125$ and $\mu_1/\mu_3 = 0.2$ are adopted, unless otherwise stated.

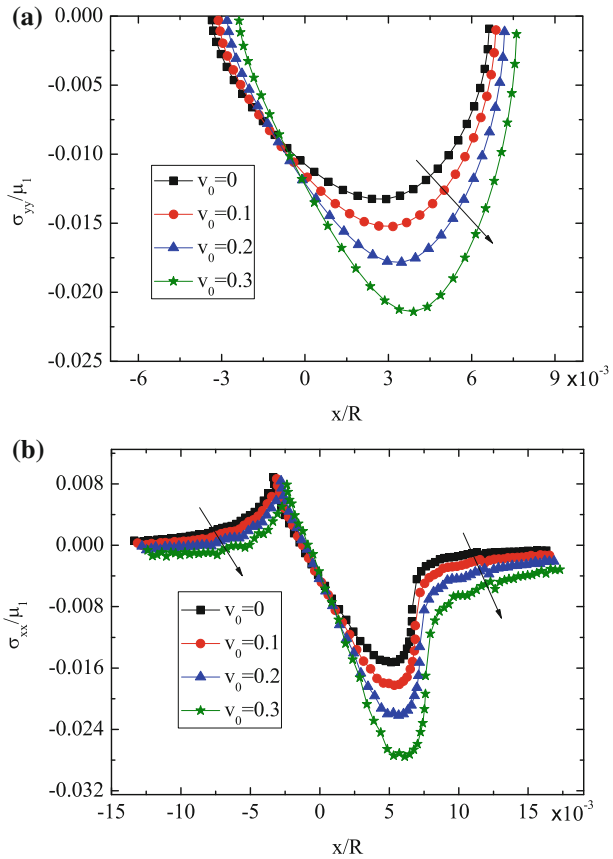

Fig. 3 Distributions of the non-dimensional contact stresses along the contact interface for different non-dimensional sliding speeds v_0 with fixed values $\mu_1/\mu_3 = 0.2$, $(a+b)/h = 1$, $R/h = 100$, $\mu_f = 0.5$. **a** For the contact pressure $\sigma_{yy}(x,0)/\mu_1$; **b** for the in-plane stress $\sigma_{xx}(x,0)/\mu_1$

According to Barber and Comninou [55], for a thermoelastic contact problem, an excessive amount of heat flux between two contact bodies may give rise to a separation of the contacting surfaces, which will change the compressive contact stress to a tensile one near the contact edges. In order to avoid such an abnormal behavior and to satisfy the perfect contact condition between the punch and the graded layer, the sliding speed of the punch should be properly controlled [2,43].

In addition, the integrals in Eqs. (63), (67) and (68) are evaluated based on the Guass-Jacobi rule, while the improper integrals in Eqs. (48a)–(48c) are calculated by means of the Guass-Legendre quadrature formula [56] with a 12-term expansion of Jacobi polynomials in Eq. (58), which has been proven to meet the solution convergence.

5.1 A special case

If the layer thickness in the present model tends to be infinity (i.e., $h \to \infty$) and the thermo effect is neglected, the problem can be reduced to a special case, that is, a rigid cylindrical punch in contact with an elastic homogeneous half-space. Closed-form solutions for the special case can be easily found from the present graded layer problem. For the reduced special model, Eq. (52) can be simplified as

$$\mu_f \Lambda_{12} p(x) + \frac{1}{\pi} \int_{-b}^{a} \frac{\Lambda_{11}}{r-x} p(r)\,\mathrm{d}r = g(x), \tag{76}$$

where

$$g(x) = \frac{x}{R}. \tag{77}$$

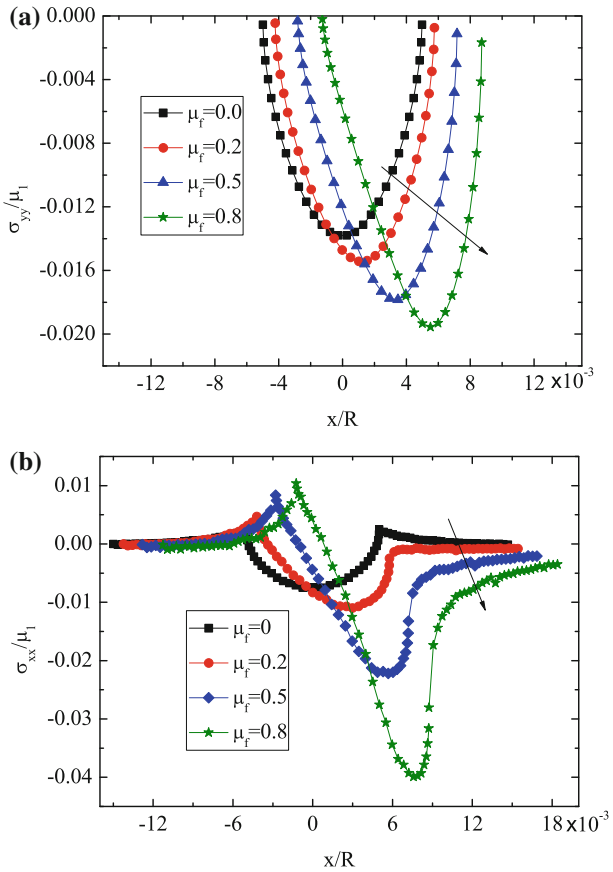

Fig. 4 Distributions of the non-dimensional contact stresses along the contact interface for different friction coefficients μ_{f} with fixed values $\mu_1/\mu_3 = 0.2$, $v_0 = 0.2$, $(a+b)/h = 1$, $R/h = 100$. **a** For the contact pressure $\sigma_{yy}(x,0)/\mu_1$; **b** for the in-plane stress $\sigma_{xx}(x,0)/\mu_1$

Solving Eq. (76) leads to the closed-form solutions

$$\frac{\sigma_{yy}(x,0)}{\mu_1} = -\frac{4}{\kappa+1}\frac{\sin\pi\beta_1}{R}(a-x)^{\beta_1}(x+b)^{\beta_2}, \tag{78}$$

$$\frac{\sigma_{xx}(x,0)}{\mu_1} = -\frac{4}{\kappa+1}\frac{\sin\pi\beta_1}{R} \times \begin{cases} (a-x)^{\beta_1}(x+b)^{\beta_2} + \frac{\mu_{\mathrm{f}}}{\pi}L_0, & -b \le x \le a, \\ \frac{\mu_{\mathrm{f}}}{\pi}L_0, & x < -b, x > a, \end{cases} \tag{79}$$

where

$$L_0(x) = \frac{\pi}{\sin\pi\beta_1}\begin{cases} -2(a-x)^{\beta_1}(-x-b)^{\beta_2} - 2x + a - b + (\beta_1-\beta_2)(a+b), & x < -b, \\ 2(a-x)^{\beta_1}(x+b)^{\beta_2}\cos\pi\beta_1 - 2x + a - b + (\beta_1-\beta_2)(a+b), & -b \le x \le a, \\ 2(x-a)^{\beta_1}(x+b)^{\beta_2} - 2x + a - b + (\beta_1-\beta_2)(a+b), & x > a, \end{cases} \tag{80}$$

and

$$a = \frac{\beta_2}{\beta_1}b. \tag{81}$$

All the results for the special case are consistent with those in [14].

5.2 Variations of the stress distribution for different parameters

From the governing equations (4)–(6) and boundary conditions (7)–(15), one can see that the solutions of the present problem depend on the ratio of shear modulus μ_1/μ_3, dimensionless sliding speed

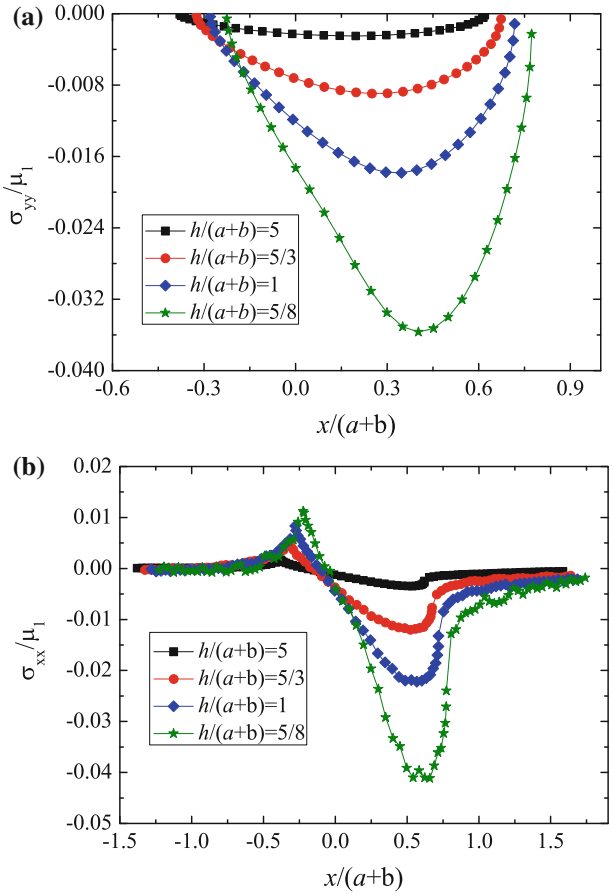

Fig. 5 Distributions of the non-dimensional contact stresses along the contact interface for different non-dimensional layer thickness $h/(a+b)$ with fixed values $\mu_1/\mu_3 = 0.2$, $v_0 = 0.2$, $\mu_f = 0.5$, $h/R = 0.01$. **a** For the contact pressure $\sigma_{yy}(x,0)/\mu_1$; **b** for the in-plane stress $\sigma_{xx}(x,0)/\mu_1$

$v_0 = \mu_1\alpha_1^* Va/k_1(\kappa+1)$, the friction coefficient μ_f and the dimensionless thickness of the graded layer $h/(a+b)$ (or the dimensionless width of contact region $(a+b)/h$).

Figure 2a, b shows the distributions of the non-dimensional interface contact pressure σ_{yy}/μ_1 and the in-plane surface stress σ_{xx}/μ_1, respectively, in which we take $(a+b)/h = 1$, $\mu_f = 0.5$, $R/h = 100$, $v_0 = 0.2$ and different ratios of shear modulus μ_1/μ_3. It is easy to find that a larger ratio of shear modulus μ_1/μ_3 results in a smaller magnitude of contact pressure in Fig. 2a, which agrees with the fact that an object with a small effective elastic modulus is easy to indent. Figure 2b clearly shows a bounded and continuous in-plane surface stress at both contact edges under a cylindrical stamp, which is different from that in a flat punch case. From Fig. 2b, one can see that, with an increasing μ_1/μ_3, the in-plane tensile surface stress behind the trailing edge improves, while the compressive one in front of the leading edge reduces. The tensile in-plane surface stress tends to induce crack initiation, which will inevitably lead to sliding surface damage. The results are qualitatively consistent with the experimental ones [9,57], where frictional sliding experiments between a steel sphere and an alumina-glass graded composite were carried out. It was found that a graded material with a 40 vol % soft glass phase at the surface could sustain a load as high as the homogeneous alumina without developing any "herringbone" crack.

The effect of the dimensionless sliding speed $v_0 = \mu_1\alpha_1^* Va/k_1(\kappa+1)$ on the distribution of contact stresses is shown in Fig. 3 with $(a+b)/h = 1$, $\mu_f = 0.5$, $R/h = 100$. The result of $v_0 = 0.0$ is also shown for comparison, which corresponds to the case without thermal effect. In Fig. 3a, the maximum of the contact stress σ_{yy} increases and the curves tend to be skew as v_0 increases. It is easy to conclude that for the same normal loading, a steady sliding of an insulating cylinder over a graded thermo-elastic layer always results in a contact width narrower than that in the corresponding isothermal case. The result shows qualitative agreement with that in Barber [36]. Furthermore, Fig. 3b shows that the maximum tensile stress σ_{xx} occurs at the

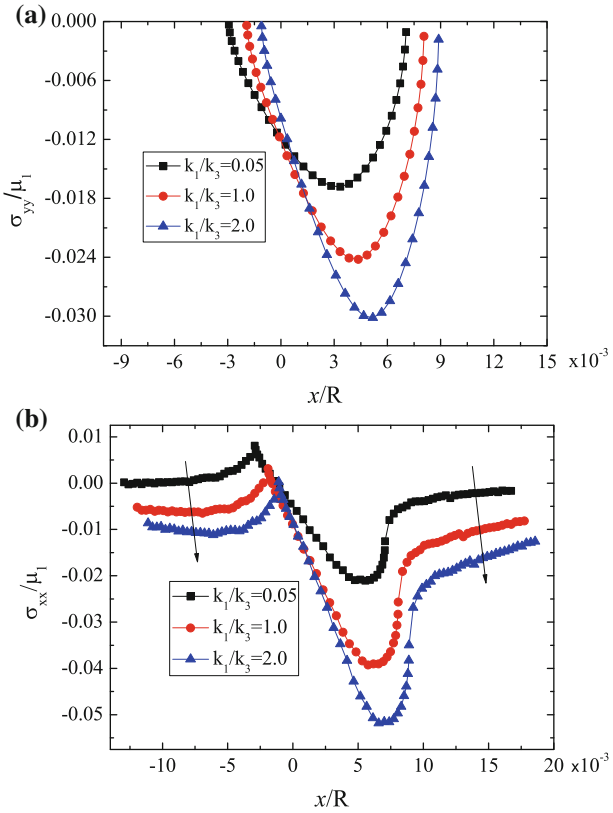

Fig. 6 Distributions of the non-dimensional contact stresses along the contact interface for different thermal conductivity ratios k_1/k_3 with fixed values $\mu_1/\mu_3 = 0.2$, $v_0 = 0.2$, $\mu_f = 0.5$, $(a+b)/h = 1$, $R/h = 100$. **a** For the contact pressure $\sigma_{yy}(x,0)/\mu_1$; **b** for the in-plane stress $\sigma_{xx}(x,0)/\mu_1$

trailing edge ($x = -b$) and decreases with an increasing v_0, which indicates a suppression tendency of the aforementioned surface crack. This phenomenon is consistent with that in [58], where it was found that the thermal effects reduced the in-plane tensile stress due to a compressive surface stress induced by the thermal effect alone. Therefore, the thermocontact damage can be suppressed by tuning the sliding speed v_0.

When the friction coefficient μ_f changes from 0.0 to 0.8, variations of the contact stress under the punch are shown in Fig. 4. One can see that, with an increasing friction coefficient μ_f, the tensile stress σ_{xx} increases sharply at the trailing edge, which indicates that a small friction coefficient is helpful to relieve thermoelastic contact damage.

Distributions of the contact pressure and the in-plane stress with different non-dimensional thickness of the graded layer $h/(a+b)$ are shown in Fig. 5a, b. Under a cylindrical punch, a decreasing ratio of $h/(a+b)$ leads to a large normal pressure. Moreover, the maximum tensile stress σ_{xx} increases with a decreasing $h/(a+b)$ implies that surface cracking happens more easily for a thinner layer case. The finding is consistent with that in Choi and Paulino [43] qualitatively, where the thermoelastic contact of a flat punch sliding over a sandwich structure, that is, a homogeneous coating on a homogeneous half-space with a graded interlayer, is considered. Furthermore, the effect of the layer thickness on the tensile stress seems much stronger in the present model than that with a graded interlayer [43].

Figures 6 and 7 are given in order to show the influence of thermal parameters on the mechanical field. The non-dimensional thermal conductivity coefficient k_1/k_3 and thermal expansion coefficient α_1/α_3 are chosen as variables, respectively. From Fig. 6a, one can see that an increasing ratio k_1/k_3 leads to a large load for a fixed $(a+b)/h$. Besides, it is interesting to find that, in Fig. 6b, the in-plane stress substantially becomes compressive with an increasing k_1/k_3, especially that behind the trailing edge ($x = -b$). It can be inferred that a higher thermal conductivity at the contact surface can prevent effectively the graded layer from crack damage during sliding friction. While Fig. 7a, b shows that the distributions of the contact pressure and in-plane stress seem insensitive to the variation of the non-dimensional thermal parameter α_1/α_3.

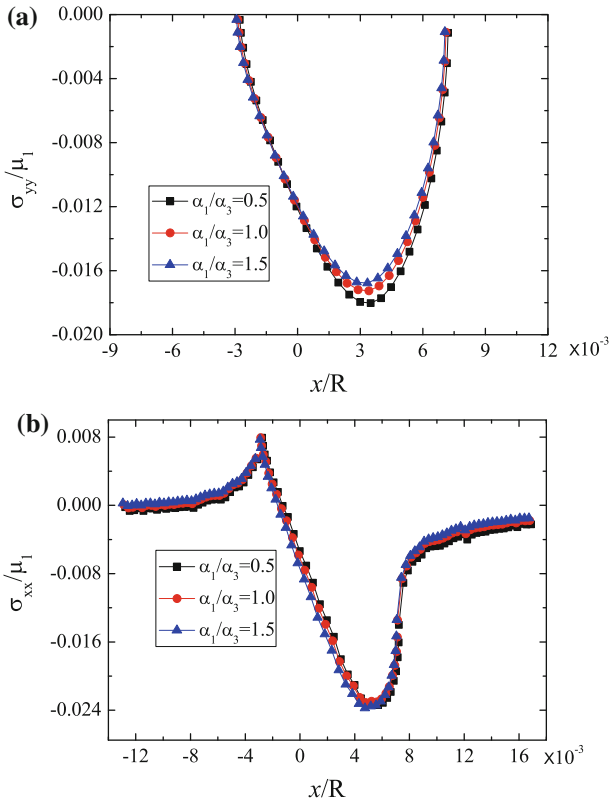

Fig. 7 Distributions of the non-dimensional contact stresses along the contact interface for different thermal expansion coefficients α_1/α_3 with fixed values $\mu_1/\mu_3 = 0.2$, $v_0 = 0.2$, $\mu_f = 0.5$, $(a+b)/h = 1$, $R/h = 100$. **a** For the contact pressure $\sigma_{yy}(x,0)/\mu_1$; **b** for the in-plane stress $\sigma_{xx}(x,0)/\mu_1$

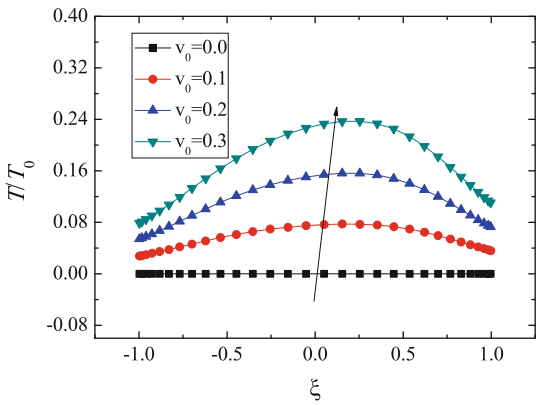

Fig. 8 Distributions of the non-dimensional temperature T/T_0 in the contact region for different non-dimensional sliding speeds v_0 with fixed values $\mu_1/\mu_3 = 0.2$, $(a+b)/h = 1$, $R/h = 100$ and $\mu_f = 0.5$, where $T_0 = \frac{\mu_* \sigma_0 k_1(\kappa+1)}{k_* \mu_1 \alpha_1^*}$

5.3 Characteristics of the surface temperature distribution

The surface temperature can be achieved with the help of the surface stresses. Figures 8, 9 and 10 present the influences of relative sliding speed v_0, friction coefficient μ_f and the dimensionless thickness of the graded layer $h/(a+b)$ on the dimensionless surface temperature distributions T/T_0, where $T_0 = \frac{\mu_* \sigma_0 k_1(\kappa+1)}{k_* \mu_1 \alpha_1^*}$ and μ_* is a typical value of friction coefficient, k_* a typical value of the thermal conductivity coefficient. In the following numerical analysis, we choose $\mu_* = 0.5$ and $k_* = 0.5$, respectively.

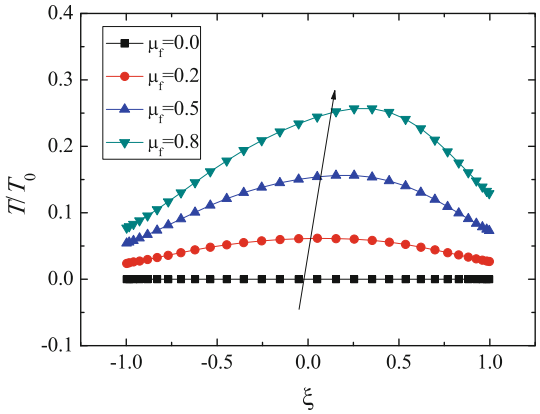

Fig. 9 Distributions of the non-dimensional temperature T/T_0 in the contact region for different friction coefficients μ_{f} with fixed values $\mu_1/\mu_3 = 0.2$, $(a+b)/h = 1$, $R/h = 100$ and $v_0 = 0.2$, where $T_0 = \frac{\mu_* \sigma_0 k_1(\kappa+1)}{k_* \mu_1 \alpha_1^*}$

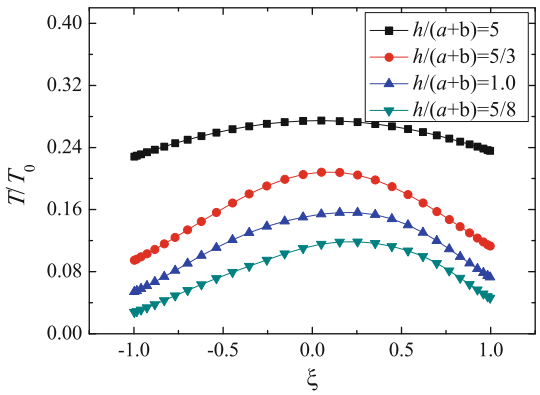

Fig. 10 Distributions of the non-dimensional temperature T/T_0 in the contact region for different non-dimensional layer thickness $h/(a+b)$ with fixed values $\mu_1/\mu_3 = 0.2$, $\mu_{\mathrm{f}} = 0.5$, $h/R = 0.01$ and $v_0 = 0.2$, where $T_0 = \frac{\mu_* \sigma_0 k_1(\kappa+1)}{k_* \mu_1 \alpha_1^*}$

Figure 8 shows the influence of v_0 on the distribution of the dimensionless surface temperature, from which one can see that the maximum surface temperature occurs near the center of the contact region due to the maximum contact stress. The surface temperature increases significantly when v_0 increases, which is because of a greater v_0 corresponding to much more heat flux generating on the contact surface. Figure 9 plots the influence of the friction coefficient μ_{f} on the distribution of the dimensionless surface temperature. It is shown that with an increasing friction coefficient, the maximum surface temperature increases sharply, which is also attributed to the increase of heat flux generation. In addition, the influence of the normalized thickness of graded layer $h/(a+b)$ on the distribution of the surface temperature is exhibited in Fig. 10, where the increase of $h/(a+b)$ induces an increasing dimensionless temperature. The increase of $h/(a+b)$ results in a decreasing material gradation parameter δ, which leads to a smaller ratio of the thermal conductivity coefficient k_2/k_1. Thus, it is much slower for the heat generated on the contact surface to flow into the graded layer, which results in an increasing surface temperature T/T_0 with an increasing thickness of the graded layer.

6 Conclusions

The features of thermo-elastic contact between a cylindrical punch and a finite graded layer are investigated. The elastic modulus, thermal conductivity coefficient and the thermal expansion coefficient of the finite graded layer vary according to different exponential laws in the thickness direction. The effects of frictional heat, friction coefficient, relative sliding speed and the thickness of the graded layer on the distributions of the contact pressure, the in-plane surface stress and the surface temperature are mainly considered. It is found that the in-plane tensile stress on the contact interface is largely responsible for the sliding-contact surface damage,

which increases with an increasing μ_1/μ_3, while it decreases with a decreasing friction coefficient, increasing sliding speed and layer thickness or an increasing thermal conductivity coefficient. During sliding, the surface temperature near the center of the contact area is slightly higher than the other regions, which increases significantly with an increasing relative sliding speed, friction coefficient and the layer thickness. Comparing to the existing literatures for a homogeneous half-space, finite boundary conditions in the present model show noteworthy influences on the stress and temperature distributions in the contact region.

It is found that, in order to prevent a finite graded layer from crack damage efficiently due to a sliding contact, several alterative methods can be adopted reasonably, such as decreasing the ratio of the surface shear modulus to the bottom one μ_1/μ_3, increasing the ratio of the surface thermal conductivity coefficient to the bottom one k_1/k_3, increasing the relative sliding speed or decreasing the friction coefficient μ_f. The results in the present paper should be useful for the design of novel graded materials in practical applications.

Acknowledgments The work reported here is supported by NSFC through Grants #10972220, #11125211, #11021262 and Nano-973-Project #2012CB937500.

References

1. Guler, M.A., Erdogan, F.: Contact mechanics of graded coatings. Int. J. Solids Struct. **41**, 3865–3889 (2004)
2. Suresh, S., Mortensen, A.: Fundamentals of Functionally Graded Materials: Processing and Thermomechanical Behaviour of Graded Metals and Metal-Ceramic Composites. Book-Institute of Materials **698** (1998)
3. Suresh, S., Giannakopoulos, A.E., Alcala, J.: Spherical indentation of compositionally graded materials: theory and experiments. Acta Mater. **45**, 1307–1321 (1997)
4. Suresh, S., Giannakopoulos, A.E., Alcala, J.: Spherical indentation of compositionally graded materials: theory and experiments. Acta Mater. **45**, 3087 (1997)
5. Jitcharoen, J., Padture, N.P., Giannakopoulos, A.E., Suresh, S.: Hertzian-crack suppression in ceramics with elastic -modulus-graded surfaces. J. Am. Ceram. Soc. **81**, 2301–2308 (1998)
6. Krumova, M., Klingshirn, C., Haupert, F., Friedrich, K.: Microhardness studies on functionally graded polymer composites. Compos. Sci. Technol. **61**, 557–563 (2001)
7. Giannakopoulos, A.E., Suresh, S.: Indentation of solids with gradients in elastic properties. 1. Point force. Int. J. Solids Struct. **34**, 2357–2392 (1997)
8. Giannakopoulos, A.E., Suresh, S.: Indentation of solids with gradients in elastic properties. 2. Axisymmetric indentors. Int. J. Solids Struct. **34**, 2393–2428 (1997)
9. Suresh, S., Olsson, M., Giannakopoulos, A.E., Padture, N.P., Jitcharoen, J.: Engineering the resistance to sliding-contact damage through controlled gradients in elastic properties at contact surfaces. Acta Mater. **47**, 3915–3926 (1999)
10. Pender, D.C., Padture, N.P., Giannakopoulos, A.E., Suresh, S.: Gradients in elastic modulus for improved contact-damage resistance. Part I: The silicon nitride-oxynitride glass system. Acta Mater. **49**, 3255–3262 (2001)
11. Pender, D.C., Thompson, S.C., Padture, N.P., Giannakopoulos, A.E., Suresh, S.: Gradients in elastic modulus for improved contact-damage resistance. Part II: The silicon nitride-silicon carbide system. Acta Mater. **49**, 3263–3268 (2001)
12. Giannakopoulos, A.E., Pallot, P.: Two-dimensional contact analysis of elastic graded materials. J. Mech. Phys. Solids **48**, 1597–1631 (2000)
13. Guler, M.A., Erdogan, F.: Contact mechanics of two deformable elastic solids with graded coatings. Mech. Mater. **38**, 633–647 (2006)
14. Guler, M.A., Erdogan, F.: The frictional sliding contact problems of rigid parabolic and cylindrical stamps on graded coatings. Int. J. Mech. Sci. **49**, 161–182 (2007)
15. Liu, T.J., Wang, Y.S.: Axisymmetric frictionless contact problem of a functionally graded coating with exponentially varying modulus. Acta Mech. **199**, 151–165 (2008)
16. Ke, L.-L., Wang, Y.-S.: Two-dimensional contact mechanics of functionally graded materials with arbitrary spatial variations of material properties. Int. J. Solids Struct. **43**, 5779–5798 (2006)
17. El-Borgi, S., Abdelmoula, R., Keer, L.: A receding contact plane problem between a functionally graded layer and a homogeneous substrate. Int. J. Solids Struct. **43**, 658–674 (2006)
18. Elloumi, R., Kallel-Kamoun, I., El-Borgi, S.: A fully coupled partial slip contact problem in a graded half-plane. Mech. Mater. **42**, 417–428 (2010)
19. Choi, H.J., Paulino, G.H.: Interfacial cracking in a graded coating/substrate system loaded by a frictional sliding flat punch. Proc. R. Soc. A-Math. Phys. Eng. Sci. **466**, 853–880 (2010)
20. Chen, S.H., Yan, C., Zhang, P., Gao, H.J.: Mechanics of adhesive contact on a power-law graded elastic half-space. J. Mech. Phys. Solids **57**, 1437–1448 (2009)
21. Chen, S.H., Chen, P.J.: Nanoadhesion of a power-law graded elastic material. Chin. Phys. Lett. **27**(10), 108102 (2010)
22. Jin, F., Guo, X.: Non-slipping adhesive contact of a rigid cylinder on an elastic power-law graded half-space. Int. J. Solids Struct. **47**, 1508–1521 (2010)
23. Guo, X., Jin, F., Gao, H.J.: Mechanics of non-slipping adhesive contact on a power-law graded elastic half-space. Int. J. Solids Struct. **48**, 2565–2575 (2011)
24. Lee, K., Barber, J.R.: Frictionally excited thermoelastic instability in automotive disk brakes. J. Tribol. **115**, 607–614 (1993)
25. Yi, Y.B., Barber, J., Hartsock, D.: Thermoelastic instabilities in automotive disc brakes-finite element analysis and experimental verification. Solid Mech. Appl. **103**, 187–202 (2002)

26. Zagrodzki, P.: Analysis of thermomechanical phenomena in multidisc clutches and brakes. Wear **140**, 291–308 (1990)
27. Zagrodzki, P., Lam, K., Al Bahkali, E., Barber, J.: Nonlinear transient behavior of a sliding system with frictionally excited thermoelastic instability. J. Tribol. **123**, 699 (2001)
28. Barik, S.P., Kanoria, M., Chaudhuri, P.K.: Steady state thermoelastic contact problem in a functionally graded material. Int. J. Eng. Sci. **46**, 775–789 (2008)
29. Jang, Y.H., Ahn, S.: Frictionally-excited thermoelastic instability in functionally graded material. Wear **262**, 1102–1112 (2007)
30. Hills, D.A., Nowell, D., Sackfield, A.: Mechanics of Elastic Contacts. Butterworth-Heinemann, Oxford (1993)
31. Pauk, V.: Plane contact problem involving heat generation and radiation. J. Theor. Appl. Mech. **32**, 829–839 (1994)
32. Pauk, V.J.: Plane contact problem for a layer involving frictional heating. Int. J. Heat Mass Transf. **42**, 2583–2589 (1999)
33. Pauk, V., Wozniak, M.: Frictional heating effects in the plane contact of layer and rigid flat punch. J. Tech. Phys. **44**, 237–244 (2003)
34. Yevtushenko, A.A., Kulchytskyzhyhailo, R.D.: Determination of limiting radii of the contact area in axisymmetrical contact problems with frictional heat-generation. J. Mech. Phys. Solids **43**, 599–604 (1995)
35. Liu, J., Ke, L.L., Wang, Y.S.: Two-dimensional thermoelastic contact problem of functionally graded materials involving frictional heating. Int. J. Solids Struct. **48**, 2536–2548 (2011)
36. Barber, J.R.: Some thermoelastic contact problems involving frictional heating. Q. J. Mech. Appl. Math. **29**, 1–13 (1976)
37. Hills, D.A., Barber, J.R.: Steady motion of an insulating rigid flat-ended punch over a thermally conducting half-plane. Wear **102**, 15–22 (1985)
38. Hills, D.A., Barber, J.R.: Steady sliding of a circular cylinder over a dissimilar thermally conducting half-plane. Int. J. Mech. Sci. **28**, 613–622 (1986)
39. Ciavarella, M., Johansson, L., Afferrante, L., Klarbring, A., Barber, J.: Interaction of thermal contact resistance and frictional heating in thermoelastic instability. Int. J. Solids Struct. **40**, 5583–5597 (2003)
40. Ciavarella, M., Barber, J.R.: Stability of thermoelastic contact for a rectangular elastic block sliding against a rigid wall. Eur. J. Mech. A-Solids **24**, 371–376 (2005)
41. Afferrante, L., Ciavarella, M.: Instability of thermoelastic contact for two half-planes sliding out-of-plane with contact resistance and frictional heating. J. Mech. Phys. Solids **52**, 1527–1547 (2004)
42. Afferrante, L., Ciavarella, M.: Separated steady state solutions for two thermoelastic half-planes in contact with out-of-plane sliding. J. Mech. Phys. Solids **53**, 1449–1475 (2005)
43. Choi, H.J., Paulino, G.H.: Thermoelastic contact mechanics for a flat punch sliding over a graded coating/substrate system with frictional heat generation. J. Mech. Phys. Solids **56**, 1673–1692 (2008)
44. Jaffar, M.J.: Frictionless contact between an elastic layer on a rigid base and a circular flat-ended punch with rounded edge or a conical punch with rounded tip. Int. J. Mech. Sci. **44**, 545–560 (2002)
45. Choi, H.J.: On the plane contact problem of a functionally graded elastic layer loaded by a frictional sliding flat punch. J. Mech. Sci. Technol. **23**, 2703–2713 (2009)
46. Li, H., Dempsey, J.P.: Axisymmetric contact of an elastic layer underlain by rigid base. Int. J. Numer. Methods Eng. **29**, 57–72 (1990)
47. Alblas, J.B., Kuipers, M.: The two dimensional contact problem of a rough stamp sliding slowly on an elastic layer—I. General considerations and thick layer asymptotics. Int. J. Solids Struct. **7**, 99–109 (1971)
48. Zhou, Y.T., Lee, K.Y.: Thermo-electro-mechanical contact behavior of a finite piezoelectric layer under a sliding punch with frictional heat generation. J. Mech. Phys. Solids **59**, 1037–1061 (2011)
49. Nowacki, W.: Thermoelasticity. Pergamon Press Ltd. **566** (1986)
50. Johnson, K.L.: Contact Mechanics. Cambridge University Press, Cambridge (1985)
51. Wang, J.H., Chen, C.Q., Lu, T.J.: Indentation responses of piezoelectric films. J. Mech. Phys. Solids **56**, 3331–3351 (2008)
52. Joachim-Ajao, D., Barber, J.R.: Effect of material properties in certain thermoelastic contact problems. J. Appl. Mech. Trans. ASME **65**, 889–893 (1998)
53. Muskhelishvili, N.L.: Singular Integral Equations. P. Noordhoff, Groningen (1953)
54. Krenk, S.: Quadrature formulas for singular integral equations of 1st and 2nd kind. Q. Appl. Math. **33**, 225–232 (1975)
55. Barber, J., Comninou, M.: Thermoelastic contact problems. Thermal Stress. **3**, 1–106 (1989)
56. Davis, P.J., Rabinowitz, P.: Methods of Numerical Integration. Academic Press, New York (1975)
57. Suresh, S.: Graded materials for resistance to contact deformation and damage. Science **292**, 2447–2451 (2001)
58. Shi, Z.: Mechanical and thermal contact analysis in layered elastic solids. Ph.D. Dissertation. University of Minnesota, vol. Ph.D. Dissertation (2001)